

## New Biomaterial Based on Cotton with Incorporated Biomolecules

Ana P. Gomes,<sup>1</sup> João F. Mano,<sup>2,3</sup> João A. Queiroz,<sup>4</sup> Isabel C. Gouveia<sup>5</sup>

<sup>1</sup>Optical Centre, University of Beira Interior, 6201-001 Covilhã, Portugal

<sup>2</sup>3B's Research Group-Biomaterials, Biodegradables, and Biomimetics, University of Minho, Headquarters of the European Institute of Excellence on Tissue Engineering and Regenerative Medicine, AvePark, 4806-909 Taipas, Guimarães, Portugal

<sup>3</sup>ICVS/3B's, PT Government Associate Laboratory, Braga/Guimarães, Portugal

<sup>4</sup>Health Sciences Research Centre, University of Beira Interior, 6201-001 Covilhã, Portugal

<sup>5</sup>R&D Unit of Textile and Paper Materials, Faculty of Engineering, University of Beira Interior, 6201-001 Covilhã, Portugal

Correspondence to: A. P. Gomes (E-mail: anapaula@ubi.pt)

**ABSTRACT:** The aim of this study was to investigate a method of embedding L-cysteine (L-cys), an antimicrobial agent, between layers of chitosan (CH) and sodium alginate (ALG) onto cotton samples obtained via a layer-by-layer electrostatic deposition technique via several embedding methods. The results show that the best way to incorporate L-cys into the layers was the one that used the property of gelling ALG. To monitor the L-cys embedding into the CH/ALG multilayer film, different methods were used: energy-dispersive X-ray spectrometry analysis to assess the presence of sulfur on the sample, Ellman's reagent method to analyze L-cys release from the sample, and attenuated total reflectance (ATR) Fourier transform infrared spectroscopy (FTIR) to compare the ATR-FTIR spectra of the pure L-cys and L-cys embedded in the CH/ALG multilayer film to study the interaction between the L-cys and the CH/ALG multilayer films. Functionalized CH/ALG cotton samples were also investigated for their antibacterial properties toward *Staphylococcus aureus* and *Klebsiella pneumonia* with the Japanese Industrial Standard method JIS L 1902:2002, and the results show an enhancement of the antibacterial effect due to the presence of L-cys. © 2014 Wiley Periodicals, Inc. *J. Appl. Polym. Sci.* **2014**, *131*, 40519.

**KEYWORDS:** biomaterials; biomedical applications; functionalization of polymers; self-assembly; textiles

Received 16 July 2013; accepted 30 January 2014

DOI: 10.1002/app.40519

### INTRODUCTION

The continuous use of antibiotics has resulted in multiresistant bacterial strains all over the world. Consequently, there is an urgent need to search for alternatives for antibiotics. For this purpose, a new strategy is proposed here: to use natural bioactive agents as potential antibacterial agents for textiles for medical applications, such as wound dressings. In this way, L-cysteine (L-cys) was used as a model to find the best strategy to introduce active agents between the layers of chitosan (CH) and sodium alginate (ALG) because L-cys is an important biomolecule, which has been extensively used in pharmaceuticals, chemical synthesis, and so on.<sup>1</sup> L-Cys can be used for the conjugation of biomolecules, and this allows it to be used for biotechnological applications.<sup>2</sup>

To deposit several layers of CH and ALG on cotton samples, a layer-by-layer (LbL) technique was used. The LbL technique offers new opportunities for the preparation of functionalized biomaterial coatings and the incorporation of bioactive molecules between the layers.<sup>3–5</sup> This technique allows the preparation of nanoarchitectures exhibiting specific properties.

Peptides, proteins, and active agents adsorbed or embedded in multilayer films have been shown to retain their biological activities,<sup>6</sup> whereas a covalent attachment to the biomaterial can reduce or even destroy their biochemical activity.<sup>5</sup> So, with the LbL technique, active agents can be directly integrated in the architecture without any covalent bonding with a biomaterial.<sup>6,7</sup>

The use of active agents coupled with polyelectrolytes constitutes a major advantage in comparison with direct chemical immobilization methods. On the other hand, the direct immobilization of active agents on a surface needs to be optimized for every individual agent/surface pair; thus, the resulting surfaces structures are much more difficult to characterize, and side reactions are detected.

An advantage of LbL is that the film can be assembled directly on the desired surface. The basic character of LbL, however, depends neither on the surface area of the support nor its shape but on the charge properties of the surface and assembling species. The layering process in LbL is repetitive and can be automated; this makes it suitable for commercial prospects in applications of technology.<sup>8</sup>

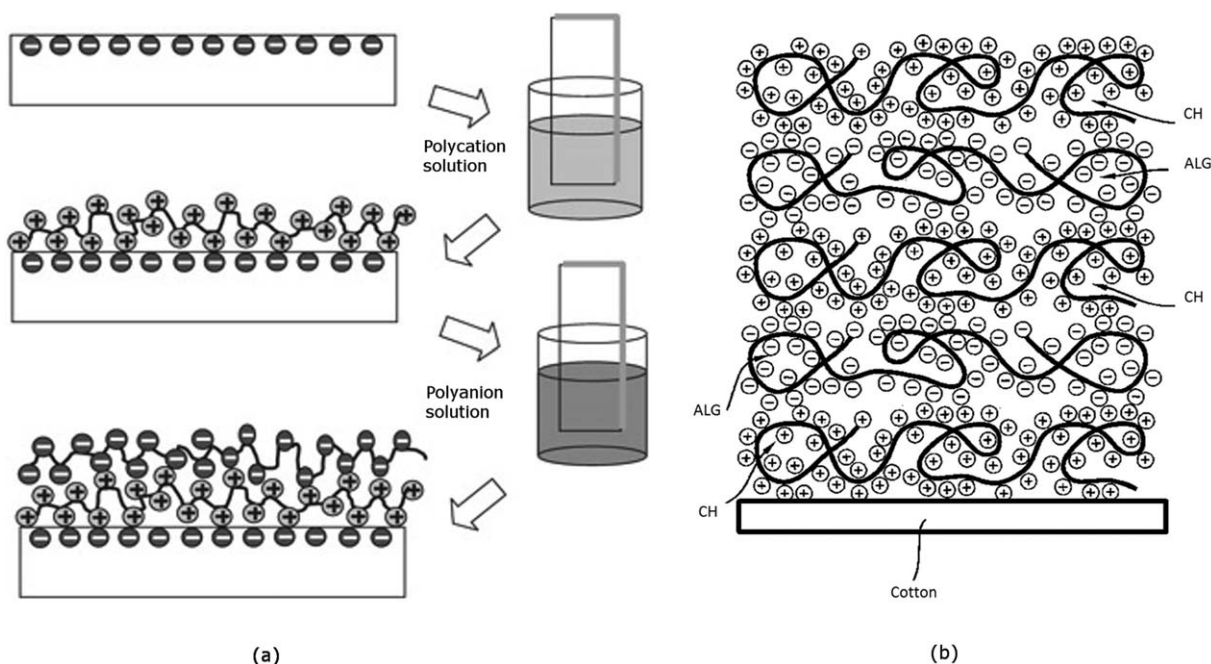


**Figure 1.** (a) Sequence of LbL electrostatic method in the negatively charged substrate with dipping into the polycationic solution (CH), deposited polycation layer, dipping into the polyanion solution (ALG), and deposited polyanion layer. (b) Structure of the functionalized sample.

The LbL method is based on the successive deposition of oppositely charged polymers onto solid surfaces,<sup>9,10</sup> as illustrated in Figure 1 (adapted from Nabok<sup>11</sup>).

The purpose of this study was to investigate the best method for the functionalization of cotton with polyelectrolyte multilayer films (CH and ALG) with incorporated L-cys. Our strategy was based on the use of multilayer films as reservoirs of active molecules. Nothing has been found in the literature concerning the aim of this study; therefore, all of the results were compared with works based on drug-delivery systems. These kinds of samples are promising examples for use in wound dressings. Natural cellulose (cotton) fiber is the basis of many wound dressings,<sup>12</sup> and wound dressings containing antibiotics have been developed for the inhibition of wound infection.<sup>13–15</sup> A variety of wound dressings that incorporate active agents is available on the market; they include iodine (Iodosorb by Smith & Nephew), chlorhexidine (Biopatch by J&J), and silver ions (Acticoat by Smith & Nephew, Actisorb by J&J, and Aquacel by ConvaTec).<sup>16</sup>

CH and ALG were selected to embed L-cys because these are natural biopolymers that are finding applications in food, cosmetics, biomedicals, and pharmaceuticals because they are biocompatible, biodegradable, and nontoxic. CH is widely used in wound dressings and has been shown to have mucoadhesive properties, a cationic nature, and antibacterial and hemostatic properties.<sup>17,18</sup> ALG is known to be nontoxic; it has hemostatic action and biocompatibility with a variety of cells. Because of these properties, ALG has been studied for application in biomaterials and wound dressings.<sup>19</sup> These natural polymers are now playing a significant role in the research field for skin, bone, vascular, nerve, and liver regeneration because of their demonstrated biocompatibility, relative abundance, and ease of processing.

ALG has the ability to form gels by reactions with divalent cations, such as  $\text{Ca}^{2+}$ . When in contact with calcium ions, ALG forms a reticulated structure that can be used to entrap drugs. ALG- $\text{RCOO}^-$  groups can bind with  $\text{Ca}^{2+}$  to form an undissolved gel. The gelling and crosslinking of the polymers are mainly achieved by the exchange of sodium ions from the guluronic acids with the divalent cations and the stacking of these guluronic groups to form the characteristic egg-box structure, as shown in Figure 2 (adapted from Shilpa et al.<sup>20</sup>).

Biodegradable dressings made of natural polymers, such as CH<sup>21,22</sup> and ALG,<sup>23</sup> are already available on the market. Specifically, biological materials such as CH and ALG have been reported to perform better than conventional and synthetic dressings in accelerating granulation tissue formation and epithelialization.<sup>22–24</sup> In this context, a new biomaterial based on cotton with incorporated active agents would be advantageous for the progressive delivery of associated active agents.

## EXPERIMENTAL

### LbL Coating of Cotton

Cotton fabric obtained from James H. Heal & Co., Ltd., was used as a substrate. (2,2,6,6-Tetramethylpiperidin-1-yl)oxyl (TEMPO)-mediated oxidation, sodium bromide (NaBr), sodium hypochlorite (NaOCl) 5%, CH (low molecular weight, 420 kDa), acetic acid ( $\text{CH}_3\text{COOH}$ ), ALG, sodium chloride (NaCl), sodium hydroxide (NaOH), and hydrochloric acid (HCl) were purchased from Sigma-Aldrich. All of the chemicals were of analytical grade and were used as received. Polyelectrolyte CH (1 mg/mL) and ALG (1 mg/mL) solutions were prepared by the dissolution of CH and ALG in 0.1M  $\text{CH}_3\text{COOH}$  and 0.5M NaCl solutions, respectively. To apply the LbL technique, samples of the substrate (cotton) were charged by immersion in a TEMPO + NaBr + 5% NaClO (pH 10.5) solution under

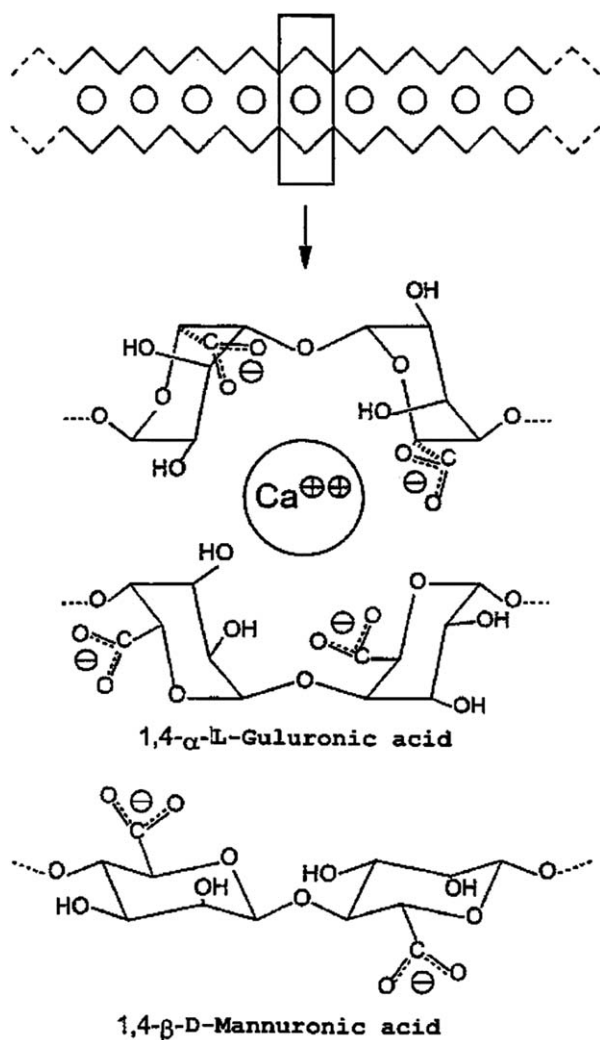


**Figure 2.** Schematic representation of an egg-box model showing the mechanism of the reaction between calcium ions and ALG that leads to gelation.

moderate stirring for 30 min; this was followed by a rinse with deionized water, as described elsewhere.<sup>25–28</sup>

The samples were manually prepared by the immersion of the cotton substrate alternately in polycation and polyanion solutions for 5 min. Between each polyelectrolyte exposure, the samples were rinsed with deionized water. For the CH and ALG polyelectrolyte layers, a pH of 5.0 was selected as an approximately intermediate value between the  $pK_a$  of CH (6.3) and the  $pK_a$  of ALG (3.38 and 3.65 for different residues).<sup>29</sup>

#### Embedding of L-Cys Between Layers

The aim of this study was to investigate a method of embedding L-cys between layers of CH and ALG deposited on cotton obtained via an LbL technique.

L-Cys was incorporated into layers of CH and ALG by different methods:

Method 1. The use of L-cys as a polyelectrolyte.

Method 2. The use of L-cys by dissolution in the polyelectrolyte.

Method 3. The introduction of L-cys by direct microspray.

Method 4. Calcium–ALG gel entrapment of L-cys.

Method 4.1. Gelling of ALG followed by immersion in the L-cys solution.

Method 4.2. Immersion in the L-cys solution followed by the gelling of ALG.

Method 4.3. Dissolution of L-cys in the gelling solution.

Method 4.4. Method 4.2 with the gelling of ALG replaced by washing with deionized water containing calcium.

Method 4.5. Method 4.4 followed by coating with CH.

Method 5. Immersion in the L-cys solution without the gelling of ALG.

**Method 1: The Use of L-Cys as a Polyelectrolyte.** The  $pK_1$  ( $-\text{COOH}$ ),  $pK_2$  (thiol or sulfhydryl), and  $pK_3$  ( $\text{NH}_3^+$ ) values of L-cys were 1.92, 8.37, and 10.70, respectively. Within a medium with a zwitterionic pH value of 5.02, there was no net charge on the molecule.<sup>3</sup> At pH values below and above 5.02, the molecule showed predominant cationic or anionic properties, respectively. With various solution pH values, the net charge could be changed from net positive at solution pH values more acidic than the isoelectric point to net negative at solution pH values more basic than the isoelectric point. At high pH values, the sulfhydryl group was also ionized and acquired a negative charge.

L-Cys was positively charged at pH 4, and this allowed it to be adsorbed onto a negative layer like a polycation. At pH 8 L-cys was negatively charged and could then be adsorbed onto a positive layer like a polyanion. Two embedding protocols were tested with the insertion of L-cys at the beginning and the end of the layer sequence considered.

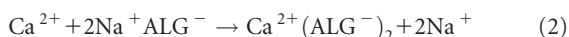
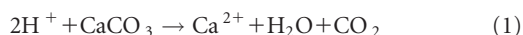
**Method 2: The Use of L-Cys by Dissolution in the Polyelectrolyte.** In this method, a small amount of L-cys (1 mg/mL) was stirred together with the anionic polyelectrolyte (ALG) and together with the cationic polyelectrolyte (CH) to keep global negative and positive charges, respectively, after dissolution.

**Method 3: Introduction of L-Cys by Direct Microspray.** In this method, L-cys was introduced between the layers of the polyelectrolyte with a microspray during the process of the LbL method to ensure the use of a very small amount of L-cys to prevent any interference with the LbL process. Two solutions of L-cys (1% w/v) were used in the microspray, one with a pH of 1 and another with a pH of 12, to ensure positive and negative charges, respectively.

**Method 4: Calcium–ALG Gel Entrapment of L-Cys.** This method consists of the immobilization of L-cys in calcium–ALG gel by entrapment. ALG has a unique ability for gel formation in the presence of divalent cations, such as calcium ions. When sodium ALG is put into a solution of calcium ions, the calcium ions replace the sodium ions in the polymer. Hydrogels based on calcium-crosslinked ALG have been widely investigated for protein drug delivery. The crosslinking between sodium ALG and calcium ions leads to the gelling and entrapment of L-cys, which are dependent on the concentrations of both of these constituents. The ALG gel showed a positive degree of swelling at low calcium concentrations and a negative degree of swelling

at higher calcium concentrations.<sup>30</sup> Therefore, the concentration of ALG and the immersion time was optimized.

Calcium carbonate [CaCO<sub>3</sub> (5%)] was suspended in deionized water, and the CaCO<sub>3</sub> particles were dispersed ultrasonically for 10 min to form a homogeneous suspension.<sup>31–33</sup> The ALG hydrogel was prepared with a CaCO<sub>3</sub> solution, and glacial CH<sub>3</sub>COOH was added to permit CaCO<sub>3</sub> solubilization. Acetic acid/CaCO<sub>3</sub> with a molar ratio of 2.5 was used.<sup>33</sup> The pH reduction (caused by proton diffusion into the aqueous phase) released Ca<sup>2+</sup> ions from the insoluble calcium complex [eq. (1)] and caused gelling [eq. (2)]:<sup>34</sup>



Taking into consideration the reaction between acetic acid and CaCO<sub>3</sub>, each mole of CaCO<sub>3</sub> reacts with 2 mol of acetic acid. A CH<sub>3</sub>COOH/CaCO<sub>3</sub> molar ratio slightly higher than the stoichiometric proportion (2.5/1) resulted in high encapsulation efficiencies.<sup>33</sup> Two different methods were applied.

**Method 4.1: Gelling of ALG Followed by Immersion in the L-Cys Solution.** After the gelling of ALG (last layer), the functionalized cotton (cotton with CH/ALG by the LbL technique) was immersed in a solution of L-cys (1% w/v) for 120 min.

**Method 4.2: Immersion in the L-Cys Solution Followed by the Gelling of ALG.** In this method, functionalized cotton was immersed in the L-cys (1% w/v) solution for 120 min, and then, the gelling of ALG was performed.

**Method 4.3: Dissolution of L-Cys in the Gelling Solution.** The functionalized cotton was immersed in a solution of (CaCO<sub>3</sub> + L-cys) to make the gelling and embedding of L-cys between the layers of CH/ALG occur simultaneously.

**Method 4.4: Method 4.2 with the Gelling of ALG Replaced by Washing with Deionized Water Containing Calcium.** The gelling process was replaced by washing with deionized water, where calcium was added. Longer exposure of ALG to the CaCO<sub>3</sub> solution induced a higher crosslinking degree, and the ALG-Ca<sup>2+</sup> network limited the repulsion of the ALG chains and, hence, decreased the maximum L-cys uptake.

Crosslinking is an effective way to stabilize three-dimensional polymer networks for a variety of applications. Different types of crosslinking are used for different applications. Covalent crosslinking has been used in hydrogel formation with permanent three-dimensional structures, such as absorbents, lubricious coatings, and even some controlled release matrices, wound dressings, and cell culture substrates.<sup>35</sup> The covalent crosslinking reagents are usually toxic to cells. In this study, we used an ionic crosslinking system without any toxic chemicals to form homogeneous ALG gels. The calcium ions had only an instant crosslinking contact with ALG to form a gel and prevent the release of L-cys.

**Method 4.5: Method 4.4 Followed by Coating with CH.** According to studies from various authors concerning the encapsulation of active agents within ALG microspheres and crosslinked CH to reinforce the microspheres,<sup>36,37</sup> we prepared samples with method 4.4, where a final CH layer was added.

**Method 5: Immersion in the L-Cys Solution Without the Gelling of ALG.** CH/ALG-functionalized cotton was immersed in a solution of L-cys (1% w/v) for 120 min.

### Morphological and Structural Characterization of the Oxidized Cotton

Untreated cotton and TEMPO oxidized cotton samples were observed with scanning electron microscopy (SEM; Hitachi S-2700). To provide surface electrical conductivity, the samples were coated with a thin Au layer, which was applied by sputtering.

The same samples were also analyzed by X-ray diffraction. A Rigaku DMAX III/C instrument was used to make a 5–50° 2θ scan with the reflection method with an operation voltage of 30 kV and a current of 20 mA. The relative crystallinity was calculated according to eq. (3).

$$\text{Relative crystallinity} = (I_{\text{crystalline}} - I_{\text{amorphous}}) \times 100\% / I_{\text{crystalline}} \quad (3)$$

where  $I_{\text{crystalline}}$  is the intensity at 22.5° and  $I_{\text{amorphous}}$  is the intensity at 18.6°.<sup>38,39</sup>

### Energy-Dispersive X-ray Spectrometry (EDS) Analysis

To monitor the L-cys embedding on the CH/ALG multilayer film, EDS analysis was used to reveal the presence of sulfur (the chemical element only present in L-cys).

### Ellman's Reagent

The amount of L-cys released from the functionalized cotton was measured by an Ellman's reagent assay. The degree of thiolation of functionalized cotton was determined by an Ellman's reagent [5,5-dithiobis(2-nitrobenzoic acid)] reaction, where 5,5-dithiobis(2-nitrobenzoic acid) reacted with thiol groups to release TNB<sup>-</sup> ions. This further ionized to TNB<sup>-2</sup>. This last ion showed a yellow color that could be detected by visible light at 405 nm.<sup>30,40</sup>

### Attenuated Total Reflectance (ATR)–Fourier Transform Infrared (FTIR) Spectra

ATR–FTIR spectra of samples were acquired on a Thermo-Nicolet is10 FTIR spectrophotometer with OMNIC software with wavelengths of 500–4000 cm<sup>-1</sup>. The spectra were collected at a resolution of 4 cm<sup>-1</sup> with 64 scans per spectrum. A background spectrum was acquired and assigned for use on subsequent spectral acquisitions for each sample.

### Assessment of Antibacterial Activity

The antibacterial effect of functionalized cotton was tested according to the Japanese Industrial Standard JIS L 1902:2002,<sup>41</sup> which is the most employed method. This method is designed to quantitatively test the ability of textiles that have been treated with antibacterial agents to prevent bacterial growth and to kill bacterial over an 18 h period of contact. This method is based on the quantitative determination of the potential effect and the activity of functionalized cotton by direct contact with a suspension of bacterial cells.

To judge the test effectiveness, the growth value ( $F$ ) was calculated according to eq. (4):

$$F = M_b - M_a \quad (4)$$

When  $F$  is more than 1.5, the test is judged to be effective, and when  $F$  is 1.5 or lower, the test is judged to be ineffective. When the test is ineffective, a retest is necessary.

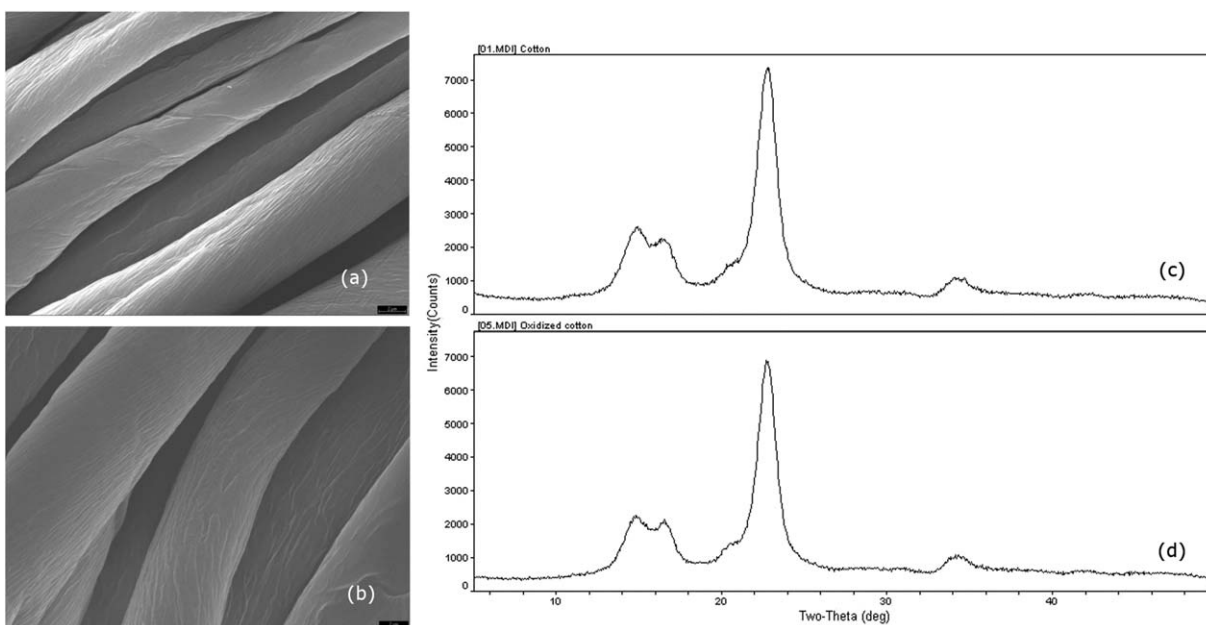


**Figure 3.** SEM images of the cotton sample (a) before and (b) after TEMPO-mediated oxidation and the corresponding X-ray diffraction patterns (c) before and (d) after TEMPO-mediated oxidation, Materials Data Inc (MDI).

When the quantitative test has been effective, the bacteriostatic activity ( $S$ ) value can be calculated in accordance with eq. (5):

$$S = M_b - M_c \quad (5)$$

The bactericidal activity ( $L$ ) was calculated according to eq. (6).

$$L = M_a - M_c \quad (6)$$

where  $M_a$  is the average common logarithm of the number of living bacteria of three test pieces immediately after the inoculation of the inoculum on standard cloth,  $M_b$  is the average common logarithm of the number of living bacteria of three test pieces after 18 h of incubation on standard cloth, and  $M_c$  is the average common logarithm of the number of living bacteria of three test pieces after 18 h of incubation on the antibacterial treated sample.<sup>41</sup> Traditionally, bacteriostatic means the prevention of multiplication of bacteria without their destruction, whereas a bactericidal effect implies the forthright killing of the organisms.<sup>42</sup>

The growth reduction rate of the bacteria was calculated with eq. (7):

$$\frac{T_{0h} - T_{18h}}{T_{0h}} \times 100\% = \text{Reduction rate (\%)} \quad (7)$$

where  $T_{0h}$  is the concentration (cfu/mL) of bacterial colonies at the initial stage (0 h) and  $T_{18h}$  is the concentration (cfu/mL) of bacterial colonies after 18 h incubation.<sup>43</sup>

## RESULTS AND DISCUSSION

### Morphological and Structural Characterization of the Oxidized Cotton

SEM images of the untreated cotton and oxidized cotton are shown in Figure 3. Figure 3(a) illustrates the original cotton sample, and the TEMPO-mediated oxidized cotton is shown in Figure 3(b).

A comparison between the SEM images of the original cotton and oxidized cotton showed that the used TEMPO-mediated oxidation conditions did not lead to any morphological change in the cotton samples.

Figure 3(c,d) illustrates the X-ray diffraction spectra of the initial cotton and oxidized cotton, respectively. Spectra are nearly identical, both in the sharpness and intensity of the diffraction. The comparison of the diffraction diagrams before and after surface oxidation indicated that the sample crystallinity was not affected by the oxidation treatment.

Comparing the original cotton samples [Figure 3(c)] with the oxidized cotton samples [Figure 3(d)], we observed that their polymorph type and crystalline degree did not show significant evolution upon the oxidation treatment. Such results agree with previously reported work.<sup>44–46</sup> The crystallinity degree of cotton was 88.06%, and the crystallinity degree of oxidized cotton was 88.50% and remained nearly constant during oxidation; this indicated that the fiber retained its crystal morphology. Generally, like other authors, we found that the process of oxidation with TEMPO did not reach the inside of the crystalline region.<sup>38,39,44</sup>

### EDS Analysis

EDS analysis obtained from the different methods of embedding L-cys between layers of CH/ALG in functionalized cotton is shown in Table I.

The existence of L-cys on the functionalized cotton samples were determined by the amount of sulfur. Samples where sulfur was not detected had no L-cys embedded between the layers; in other words, the method used did not work. As shown in Table I, methods 1, 2, and 3 did not work because L-cys was not retained between the layers. That is, there were no

**Table I.** Results of the Embedding of L-Cys

Method <sup>a</sup>	Sample	Sequence	L-Cys pH	Sulfur (wt %)
1	1	Cotton-CH-ALG-(L-cys)-ALG-CH-ALG	4	—
1	2	Cotton-CH-ALG-CH-ALG-(L-cys)-ALG	4	—
1	3	Cotton-CH-(L-cys)-CH-ALG-CH-ALG	8	—
1	4	Cotton-CH-ALG-CH-(L-cys)-CH-ALG	8	—
2	5	Cotton-CH-(ALG+L-cys)-CH-ALG-CH-ALG	—	—
2	6	Cotton-CH-ALG-CH-(ALG+L-cys)-CH-ALG	—	—
2	7	Cotton-(CH+L-cys)-ALG-CH-ALG-CH-ALG	—	—
2	8	Cotton-CH-ALG-(CH+L-cys)-ALG-CH-ALG	—	—
3	9	Cotton-CH-ALG-(spray L-cys)-CH-ALG-CH-ALG	1	—
3	10	Cotton-CH-(spray L-cys)-ALG-CH-ALG-CH-ALG	12	—
3	11	Cotton-CH-ALG-CH-ALG-CH-(spray L-cys)-ALG	12	—
3	12	Cotton-CH-ALG-CH-ALG-(spray L-cys)-CH-ALG	1	—
4.1	13	Cotton-CH-ALG-gelation-L-cys (1%w/v, 120 min)	—	0.42
4.2	14	Cotton-CH-ALG-L-cys (1%w/v, 120 min)- gelation	—	0.70
4.3	15	Cotton-CH-ALG- gelation (CaCO <sub>3</sub> +L-cys)	—	0.18
4.4	16	Cotton-CH-ALG- L-cys (1% w/v, 120 min)-wash (water with CaCO <sub>3</sub> )	—	0.90
4.5	17	Cotton-CH-ALG-L-cys (1% w/v, 120 min)-wash (water with CaCO <sub>3</sub> )-CH	—	0.85
5	18	Cotton-CH-ALG-L-cys (1% w/v, 120 min)	—	0.09

<sup>a</sup>1, With L-cys as the polyelectrolyte; 2, with L-cys by dissolution in the polyelectrolyte; 3, introduction of L-cys by direct microspray; 4.1, gelation of ALG followed by immersion in an L-cys solution; 4.2, immersion in L-cys solution followed by the gelation of ALG; 4.3, dissolution of L-cys in the gelation solution; 4.4, method 4.2 with the gelation of ALG replaced by washing with deionized water containing calcium; 4.5, method 4.4 followed by coating with CH; 5, immersion in L-cys solution without the gelation of ALG.

electrostatic interactions between L-cys and CH and ALG. L-Cys is free and comes out easily during the LbL process. The result obtained by method 2 was in accordance with the results of the literature for drugs incorporated in biodegradable ALG.<sup>47</sup> The dissolution of the drug in polyelectrolyte led to good results when the drug was insoluble in water. Water-soluble drugs (in the case of L-cys) are not suitable for this technique because of the rapid loss of the external phase.<sup>48</sup>

In methods 4.1, 4.2, 4.3, 4.4, and 4.5, the presence of sulfur was detected. It was clear that the best result occurred when there was gelling. In method 4.3, there was less incorporation of L-cys compared with methods 4.1, 4.2, 4.4, and 4.5. The dissolution of L-cys (method 4.3) in the gelling solution interfered with the gelling process, and this resulted in lower values of incorporation of L-cys. The decrease in the L-cys content was a result of L-cys diffusion through the crosslinked ALG gel into the CaCO<sub>3</sub> solution. Comparing the results between methods 4.1 and 4.2 and methods 4.4 and 4.5, we observed that the process of gelling was not necessary because the addition of calcium in the wash water solution was enough to obtain desirable entrapment. Longer exposure of the ALG to the CaCO<sub>3</sub> solution induced a higher crosslinking degree, and the ALG-Ca<sup>2+</sup> network limited the repulsion of the ALG chains and decreased the maximum L-cys uptake capacity. This evidence agreed with the results reported by Smrdel et al.,<sup>49</sup> where after 1 min of hardening, only the surface was cross-linked, whereas the interior of the beads was still liquid. On

the other hand, a higher concentration of CaCO<sub>3</sub> resulted in a denser network; this prevented the ALG from eroding out of the film and delayed the kinetics of L-cys release.<sup>50</sup>

Method 4.4 led to better results with the greatest amount of detected sulfur; this meant that there was a larger amount of L-cys embedded between the CH/ALG layers.

In method 5, a very low amount of sulfur was detected. This indicated that a very small amount of L-cys was embedded between the layers of CH/ALG. In this method, gelling was not used, and a very low amount of L-cys between the layers was detected. This suggested that the gelling process was essential for the incorporation of L-cys between the layers of CH/ALG.

#### Ellman's Reagent

Samples 16 and 17 (samples with better results of L-cys incorporation, see Table I) were immersed in deionized water. Small amounts of liquid solution were collected and replenished by fresh deionized water and analyzed for different immersion times. The results for the absorbance obtained by the method of Ellman's reagent are shown in Figure 4.

After immersion for 90 min in deionized water, the result of EDS analysis by weight percentage for sample 16 was 0.40% in sulfur and for sample 17 was 0.37% in sulfur. There was a reduction of 50% in the content of sulfur in each sample; this suggested that there was a release of 50% of L-cys for an immersion time of 90 min.

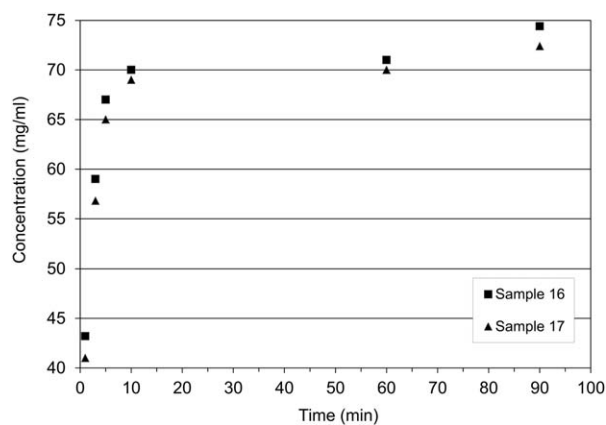


Figure 4. Ellman's reagent.

### ATR-FTIR Spectra

Figure 5(a,b) shows characteristic cellulose peaks around  $1000\text{--}1200\text{ cm}^{-1}$ , which were those of the main components of cotton. Other characteristic bands related to the chemical structure of cellulose were hydrogen-bonded OH stretching around  $3100\text{--}3550\text{ cm}^{-1}$ , C—H stretching around  $2800\text{ cm}^{-1}$ , and asymmetrical  $\text{COO}^-$  stretching around  $1600\text{ cm}^{-1}$ .<sup>51–53</sup> The characteristic peaks of CH were detected in the region around  $1700\text{--}1500\text{ cm}^{-1}$  and corresponded to amino groups. The ALG spectrum showed the characteristic bands of carboxylate ( $\text{COO}^-$ ) at  $1600$  and  $1400\text{ cm}^{-1}$ .<sup>54</sup>

Pure L-cys showed bands at  $1575$  and  $1390\text{ cm}^{-1}$  corresponding to the asymmetric and symmetric stretching of  $\text{COO}^-$ .<sup>55</sup> Characteristic peaks for L-cys resulting from amine bending vibrations modes were observed at  $1523$  and  $1420\text{ cm}^{-1}$ .<sup>55</sup> The peak at  $2551\text{ cm}^{-1}$  corresponded to the —SH group (thiol group of L-cys).<sup>56</sup> Figure 5(b) shows the spectrum of the functionalized cotton sample with L-cys, where the absence of the —SH band at  $2551\text{ cm}^{-1}$ . This indicated sulfur–hydrogen bond breakage, and a new sulfur–sulfur bond appeared at  $558\text{ cm}^{-1}$ .<sup>2,57</sup>

Comparing Figure 5(a) and 5(b), we observed that the curves were similar and had no displacement in the appearance of peaks. This indicated that there was no chemical bond between CH/ALG and L-cys. The absence of chemical bonds suggested that L-cys may have been coordinated with the nitrogen of the amino group of CH and the oxygen of the carboxylate group of ALG.

### Best Configuration for the Samples

Considering all the results obtained in this study and the results reported in an already published article,<sup>58</sup> we found that five layers was the best setting for functionalized cotton with CH and ALG. So, the best settings in the preparation of the functionalized cotton were

Sample 19: Cotton–CH–ALG–CH–ALG–L-cys (1% w/v, 120 min)–wash (water with  $\text{CaCO}_3$ ).

Sample 20: Cotton–CH–ALG–CH–ALG–L-cys (1% w/v, 120 min)–wash (water with  $\text{CaCO}_3$ )–CH.

### Assessment of Antibacterial Activity

Table II presents the values of bacteriostatic and bactericidal activity levels for samples 19, 19 control, 20, and 20 control.

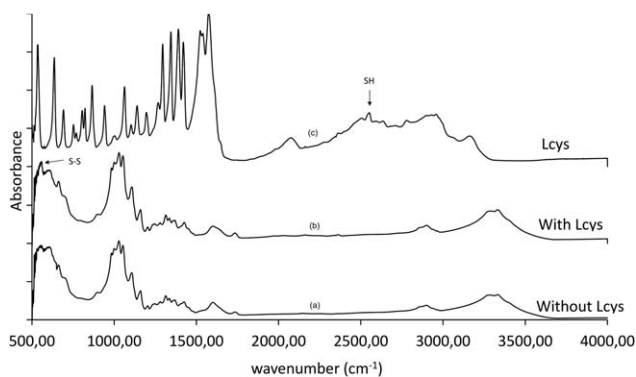


Figure 5. ATR-FTIR spectra of (a) a functionalized cotton sample with CH/ALG and without L-cys, (b) a functionalized cotton sample with CH/ALG and L-cys incorporated, and (c) L-cys.

The control samples had the same configuration of samples 19 and 20 but without immersion in the L-cys solution.

All samples (19, 19 control, 20, and 20 control) showed bacteriostatic activity and no bactericidal activity against *Staphylococcus aureus* and *Klebsiella pneumoniae*.

For *S. aureus*, the bacteriostatic activity level in sample 19 (with L-cys) increased approximately 70% relative to the sample 19 control (without L-cys). Similarly, the bacteriostatic activity level in sample 20 (with L-cys) increased approximately 60% relative to the sample 20 control (without L-cys). For the *K. pneumoniae*, the behavior was similar to the previous one, so the bacteriostatic activity level in sample 19 (with L-cys) increased approximately 90% relative to the sample 19 control (without L-cys). For sample 20 (with L-cys), the bacteriostatic activity level increased approximately 80% relative to the sample 20 control (without L-cys). By analyzing these results, we found that the presence of L-cys in the sample significantly increased the bacteriostatic activity level.

Sample 20 presented the highest values of bacteriostatic activity (2.9 for *S. aureus* and 2.2 for *K. pneumoniae*). The last layer in this sample was composed of CH. Normally, CH exhibits a stronger bioactivity effect upon Gram-positive (*S. aureus*) and Gram-negative (*K. pneumoniae*) bacteria.<sup>59,60</sup> This fact may be explained by the number of amine groups available for reaction. CH is a cation that will attract the negative charges of the cell

Table II. Bacteriostatic and Bactericidal Activity

Sample	<i>S. aureus</i>		<i>K. pneumoniae</i>	
	$M_b - M_c$	$M_a - M_c$	$M_b - M_c$	$M_a - M_c$
19	2.1	−0.2	1.9	−0.3
19 control	1.2	−0.6	1.0	−0.6
20	2.9	−0.1	2.2	−0.2
20 control	1.8	−0.4	1.2	−0.8

A, number of inoculated bacteria; B, number of bacteria on the standard sample contacted for 18 h; C, number of bacteria on the functionalized sample after incubation for 18 h.  $M_a = \log A$ ,  $M_b = \log B$ ,  $M_c = \log C$ . Bacteriostatic activity level =  $M_b - M_c$ . Bactericidal activity level =  $M_a - M_c$ .

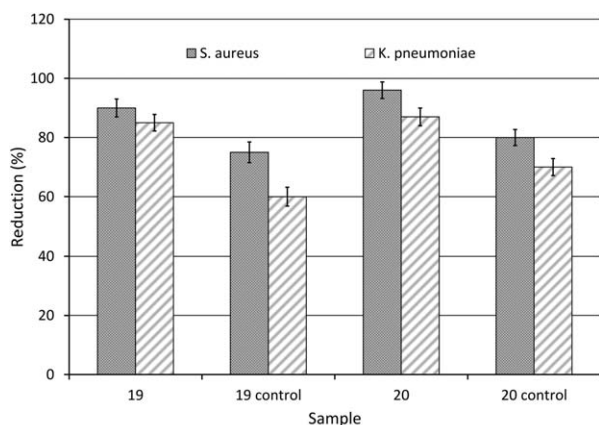


**Figure 6.** Reduction rate percentages of *S. aureus* and *K. pneumoniae* in the functionalized samples with L-cys incorporated.

walls of bacteria and cause damage and sometimes even death.<sup>61–64</sup>

The sample 20 control presented lower values of bacteriostatic activity (1.8 for *S. aureus* and 1.2 for *K. pneumoniae*) with respect to sample 20. These values were due to the layers of CH and ALG, which had antibacterial properties, but otherwise, there was no L-cys in this sample. This suggested that L-cys conferred a greater antibacterial effect to the samples.

Sample 19 presented values of bacteriostatic activity of 2.1 for *S. aureus* and 1.9 for *K. pneumoniae*. As expected, the sample 19 control had lower values for bacteriostatic activity (1.2 for *S. aureus* and 1.0 for *K. pneumoniae*) because it had no L-cys.

Figure 6 shows the growth inhibition (cell reduction) of *S. aureus* and *K. pneumoniae* by antibacterial activity of the functionalized cotton with L-cys incorporated.

Analyzing the results (Figure 6) for *S. aureus*, we found a reduction of 90% in bacterial growth on sample 19 and a reduction of 95% on sample 20. For *K. pneumoniae*, there was a reduction of 84% in bacterial growth on sample 19 and a reduction of 87% on sample 20.

For the 19 and 20 control samples for *S. aureus*, there were reductions of 72 and 80% in bacterial growth, respectively. For *K. pneumoniae*, there were reductions of 60 and 70% in bacterial growth on the 19 and 20 control samples, respectively.

Sample 20 presented a greater reduction in bacterial growth than sample 19. This difference was due to the presence of CH in the last layer of sample 20. As discussed in an article already published<sup>58</sup> and based on the literature, CH exhibited a stronger bioactivity effect upon *S. aureus* and *K. pneumoniae* bacteria.

From Figure 6, the difference in values was explained by the presence of L-cys in samples 19 and 20. The presence of L-cys gave a higher antibacterial activity to the functionalized cotton samples.

## CONCLUSIONS

L-Cys, a bioactive agent, could be directly embedded between the layers of CH/ALG without any covalent bonding with a polyelec-

trolyte. With the results obtained taken into account, method 4.4 or 4.5 would be the most appropriate for that purpose. This method has many advantages; in particular, the bioactive agent was immobilized between layers (no chemical bond) without the necessary optimization for each bioactive agent because the agent could be embedded by methods 4.4 or 4.5.

In addition, LbL deposition allows the easy fabrication of multi-material films, in which different layers carry different functionalities or repeat the same functionality several times to control the quality or the quantity of active agents.

Our results strongly suggest that biofunctionalized polyelectrolyte multilayered films containing L-cys represent a promising area for development in biomaterials and biotechnology. Thus, these unique structures are potentially very useful as wound dressings.

## ACKNOWLEDGMENTS

The authors thank Fundação para a Ciência e Tecnologia for the funding granted concerning the project PTDC/EBB-BIO/113671/2009 (FCOMP-01-0124-FEDER-014752). Also, they thank Fundo Europeu de Desenvolvimento Regional through COMPETE—Programa Operacional Factores de Competitividade for cofunding.

## REFERENCES

- Caldeira, E.; Piskin, E.; Granadeiro, L.; Silva, F.; Gouveia, I. *C. J. Biotechnol.* **2013**, *168*, 426.
- Feliciano-Ramos, I.; Caban-Acevedo, M.; Scibioh, M. A.; Cabrera, C. R. *J. Electroanal. Chem.* **2010**, *650*, 98.
- Sanders, W.; Anderson, M. R. *J. Colloid Interface Sci.* **2009**, *331*, 318.
- Pedrosa, V. A.; Paixao, T. R. L. C.; Freire, R. S.; Bertotti, M. *J. Electroanal. Chem.* **2007**, *602*, 149.
- Martins, G. V.; Merino, E. G.; Mano, J. F.; Alves, N. M. *Macromol. Biosci.* **2010**, *10*, 1444.
- Leguen, E.; Chassepot, A.; Decher, G.; Schaaf, P.; Voegel, J. C.; Jessel, N. *Biomol. Eng.* **2007**, *24*, 33.
- Macdonald, M. L.; Samuel, R. E.; Shah, N. J.; Padera, R. F.; Beben, Y. M.; Hammond, P. T. *Biomaterials* **2011**, *32*, 1446.
- Rudra, J. S.; Dave, K.; Haynie, D. T. *J. Biomater. Sci. Polym. Ed.* **2006**, *17*, 1301.
- Decher, G.; Hong, J. D.; Schmitt, J. *Thin Solid Films* **1992**, *210*, 831.
- Lvov, Y.; Decher, G.; Mohwald, H. *Langmuir* **1993**, *9*, 481.
- Nabok, A. *Organic and Inorganic Nanostructures*; Artech House: Boston, **2005**.
- Dong, H.; Hinestroza, J. P. *ACS Appl. Mater. Interfaces* **2009**, *1*, 797.
- Wang, Y. C.; Lin, M. C.; Wang, D. M.; Hsieh, H. *J. Biomaterials* **2003**, *24*, 1047.
- Rujitanaroj, P. O.; Pimpha, N.; Supaphol, P. *Polymer* **2008**, *49*, 4723.
- Dong, Y.; Liu, H. Z.; Xu, L.; Li, G.; Ma, Z. N.; Han, F.; Yao, H. M.; Sun, Y. H.; Li, S. M. *Chin. Chem. Lett.* **2010**, *21*, 1011.



16. Elsner, J. J.; Berdichevsky, I.; Zilberman, M. *Acta Biomater.* **2011**, *7*, 325.
17. Alves, N. M.; Picart, C.; Mano, J. F. *Macromol. Biosci.* **2009**, *9*, 776.
18. Jayakumar, R.; Chennazhi, K. P.; Muzzarelli, R. A. A.; Tamura, H.; Nair, S. V.; Selvamurugan, N. *Carbohydr. Polym.* **2010**, *79*, 1.
19. de Moraes, M. A.; Beppu, M. M. *J. Appl. Polym. Sci.* **2013**, *130*, 3451.
20. Shilpa, A.; Agrawal, S. S.; Ray, A. R. *J. Macromol. Sci. Polym. Rev.* **2003**, *43*, 187.
21. Zilberman, M.; Elsner, J. J. *J. Controlled Release* **2008**, *130*, 202.
22. Campos, M. G. N.; Rawls, H. R.; Innocentini-Mei, L. H.; Satsangi, N. *J. Mater. Sci. Mater. Med.* **2009**, *20*, 537.
23. Suzuki, Y.; Tanihara, M.; Nishimura, Y.; Suzuki, K.; Yamawaki, Y.; Kudo, H.; Kakimaru, Y.; Shimizu, Y. *J. Biomed. Mater. Res.* **1999**, *48*, 522.
24. Takeoka, S.; Okamura, Y.; Fujie, T.; Fukui, Y. *Pure Appl. Chem.* **2008**, *80*, 2259.
25. Saito, T.; Okita, Y.; Nge, T. T.; Sugiyama, J.; Isogai, A. *Carbohydr. Polym.* **2006**, *65*, 435.
26. Dang, Z.; Zhang, J. G.; Ragauskas, A. *J. Carbohydr. Polym.* **2007**, *70*, 310.
27. Diez, I.; Eronen, P.; Osterberg, M.; Linder, M. B.; Ikkala, O.; Ras, R. H. A. *Macromol. Biosci.* **2011**, *11*, 1185.
28. Gomes, A. P.; Mano, J. F.; Queiroz, J. A.; Gouveia, I. C. *J. Polym. Environ.* **2012**, *20*, 1084.
29. Maurstad, G.; Morch, Y. A.; Bausch, A. R.; Stokke, B. T. *Carbohydr. Polym.* **2008**, *71*, 672.
30. Davidovich-Pinhas, M.; Harari, O.; Bianco-Peled, H. *J. Controlled Release* **2009**, *136*, 38.
31. Ribeiro, A. J.; Neufeld, R. J.; Arnaud, P.; Chaumeil, J. C. *Int. J. Pharm.* **1999**, *187*, 115.
32. Silva, C. M.; Ribeiro, A. J.; Ferreira, D.; Veiga, F. *Eur. J. Pharm. Sci.* **2006**, *29*, 148.
33. Silva, C. M.; Ribeiro, A. J.; Figueiredo, M.; Ferreira, D.; Veiga, F. *AAPS J.* **2005**, *7*, E903.
34. Tan, W. H.; Takeuchi, S. *Adv. Mater.* **2007**, *19*, 2696.
35. Kuo, C. K.; Ma, P. X. *Biomaterials* **2001**, *22*, 511.
36. Alexakis, T.; Boadi, D. K.; Quong, D.; Groboillot, A.; Oneill, I.; Poncellet, D.; Neufeld, R. *J. Appl. Biochem. Biotechnol.* **1995**, *50*, 93.
37. Kafshgari, M. H.; Khorram, M.; Khodadoost, M.; Khavari, S. *Iran. Polym. J.* **2011**, *20*, 445.
38. Qin, Z. Y.; Tong, G. L.; Chin, Y. C. F.; Zhou, J. C. *Bioresources* **2011**, *6*, 1136.
39. Dai, L.; Dai, H. Q.; Yuan, Y. C.; Sun, X.; Zhu, Z. *J. Biore-sources* **2011**, *6*, 2619.
40. Gouveia, I. C.; Sa, D.; Henriques, M. *J. Appl. Polym. Sci.* **2012**, *124*, 1352.
41. Testing for Antibacterial Activity and Efficacy on Textile Products; Japanese Industrial Standard JIS L 1902:2002; Japanese Standards Association: Tokyo, **2002**.
42. Pankey, G. A.; Sabath, L. D. *Clin. Infect. Dis.* **2004**, *38*, 864.
43. Park, S. J.; Park, Y. M. *Fiber Polym.* **2010**, *11*, 357.
44. Saito, T.; Isogai, A. *Biomacromolecules* **2004**, *5*, 1983.
45. Habibi, Y.; Chanzy, H.; Vignon, M. R. *Cellulose* **2006**, *13*, 679.
46. Montanari, S.; Rountani, M.; Heux, L.; Vignon, M. R. *Macromolecules* **2005**, *38*, 1665.
47. Sevgi, F.; Kaynarsoy, B.; Ertan, G. *Pharm. Dev. Technol.* **2008**, *13*, 5.
48. Bodmeier, R.; Oh, K. H.; Prammar, Y. *Drug Dev. Ind. Pharm.* **1989**, *15*, 1475.
49. Smrdel, P.; Bogataj, M.; Podlogar, F.; Planinsek, O.; Zajc, N.; Mazaj, M.; Kaucic, V.; Mrhar, A. *Drug Dev. Ind. Pharm.* **2006**, *32*, 623.
50. Wang, P.; Fan, X. R.; Cui, L.; Wang, Q.; Zhou, A. H. *J. Environ. Sci. China* **2008**, *20*, 1519.
51. Yan, H. J.; Hua, Z. Z.; Qian, G. S.; Wang, M.; Du, G. C.; Chen, J. *Cellulose* **2009**, *16*, 1099.
52. Chung, C.; Lee, M.; Choe, E. K. *Carbohydr. Polym.* **2004**, *58*, 417.
53. Wang, Q.; Fan, X. R.; Gao, W. D.; Chen, J. *Carbohydr. Res.* **2006**, *341*, 2170.
54. Deng, H. B.; Zhou, X.; Wang, X. Y.; Zhang, C. Y.; Ding, B.; Zhang, Q. H.; Du, Y. M. *Carbohydr. Polym.* **2010**, *80*, 474.
55. Varghese, M. V.; Dhumal, R. S.; Patil, S. S.; Paradkar, A. R.; Khanna, P. K. *Synth. React. Inorg. Met.* **2009**, *39*, 554.
56. Shao, J.; Yang, Y. M.; Shi, C. G. *J. Appl. Polym. Sci.* **2003**, *88*, 2575.
57. Wolpert, M.; Hellwig, P. *Spectrochim. Acta A* **2006**, *64*, 987.
58. Gomes, A. P.; Mano, J. F.; Queiroz, J. A.; Gouveia, I. C. *Polym. Adv. Technol.* **2013**, *24*, 1005.
59. Fernandes, J. C.; Tavaría, F. K.; Fonseca, S. C.; Ramos, O. S.; Pintado, M. E.; Malcata, F. X. *J. Microbiol. Biotechnol.* **2010**, *20*, 311.
60. No, H. K.; Park, N. Y.; Lee, S. H.; Meyers, S. P. *Int. J. Food Microbiol.* **2002**, *74*, 65.
61. Qi, L. F.; Xu, Z. R.; Jiang, X.; Hu, C. H.; Zou, X. F. *Carbohydr. Res.* **2004**, *339*, 2693.
62. Wang, X. H.; Du, Y. M.; Fan, L. H.; Liu, H.; Hu, Y. *Polym. Bull.* **2005**, *55*, 105.
63. Hsieh, S. H.; Ciou, J. H.; Wang, J. J. *J. Appl. Polym. Sci.* **2007**, *103*, 4080.
64. Chung, Y. C.; Chen, C. Y. *Bioresour. Technol.* **2008**, *99*, 2806.